SUPPLEMENTARY DATA

Supplementary Figure 1. Visualization of endoplasmic reticulum-mitochondria interaction by *in situ* proximity ligation assay. A) Illustration of targeted proteins in mitochondria (M), endoplasmic reticulum (ER) or MAM interface. B) Schematic illustration of the detection of ER-mitochondria interactions by *in situ* PLA : a) mouse primary antibody directed against VDAC1 and rabbit primary antibody directed against IP3R1can bind in proximity at MAM interface, b) upon addition of PLA probes directed against mouse and rabbit IgG, their attached DNA strands form templates for ligation of connector oligos, c) the circular DNA Strand that is formed can be amplified and d) visualized by microscopy as a fluorescent spot using texas red–labeled oligonucleotides.

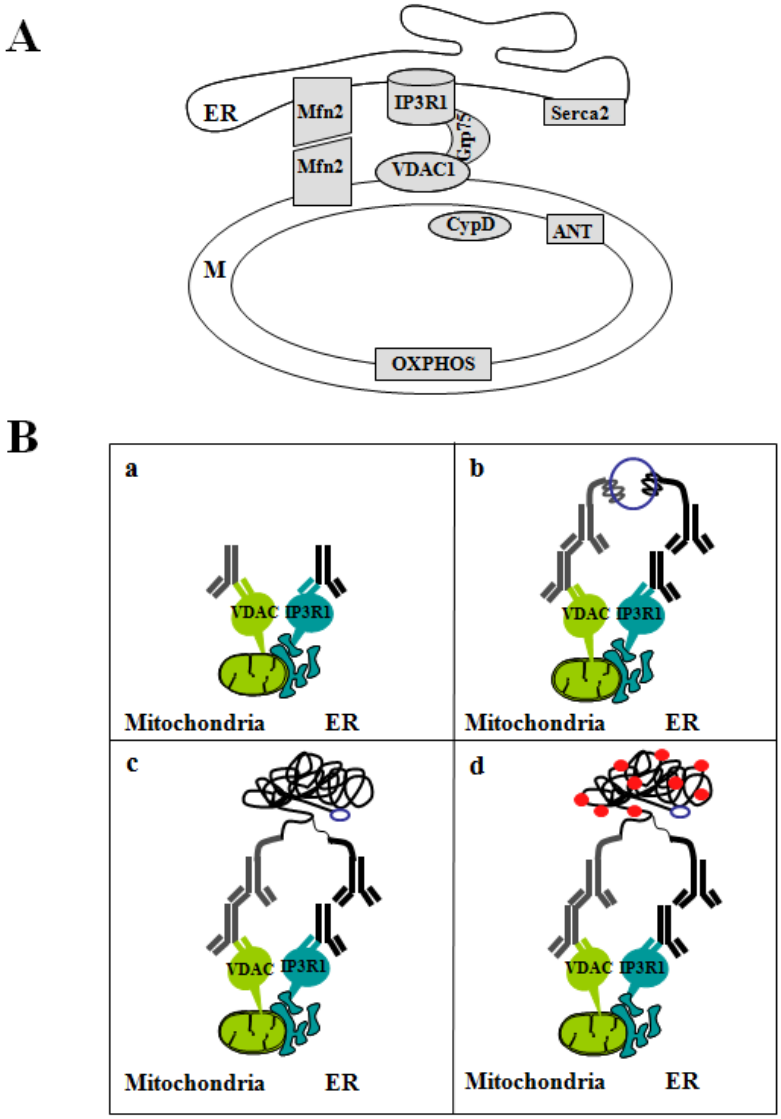

SUPPLEMENTARY DATA

Supplementary Figure 2. Validation of the primary antibodies used in *in situ* PLA experiments. A) Representative Western blots illustrating inhibition or overexpression of specific proteins (VDAC1, Grp75, IP3R1, Mfn2) after siRNA silencing or transient transfection experiments. HuH7 cells transfected with specific siRNA for VDAC1, Grp75, IP3R1 or Mfn2 show reduced expression of their protein levels compared to control cells, whereas cells tranfected with transient transfection vectors for Mfn2 and Grp75 show Increased expression of their proteins. B) Immuno-fluorescence illustrating co-localization (in yellow) of mitochondrial (VDAC1 and OXPHOS) or ER (Serca2 and IP3R1) proteins (x63 and scale bar=20mm). Nuclei appear in blue. At right, a zoom of merged images is shown.

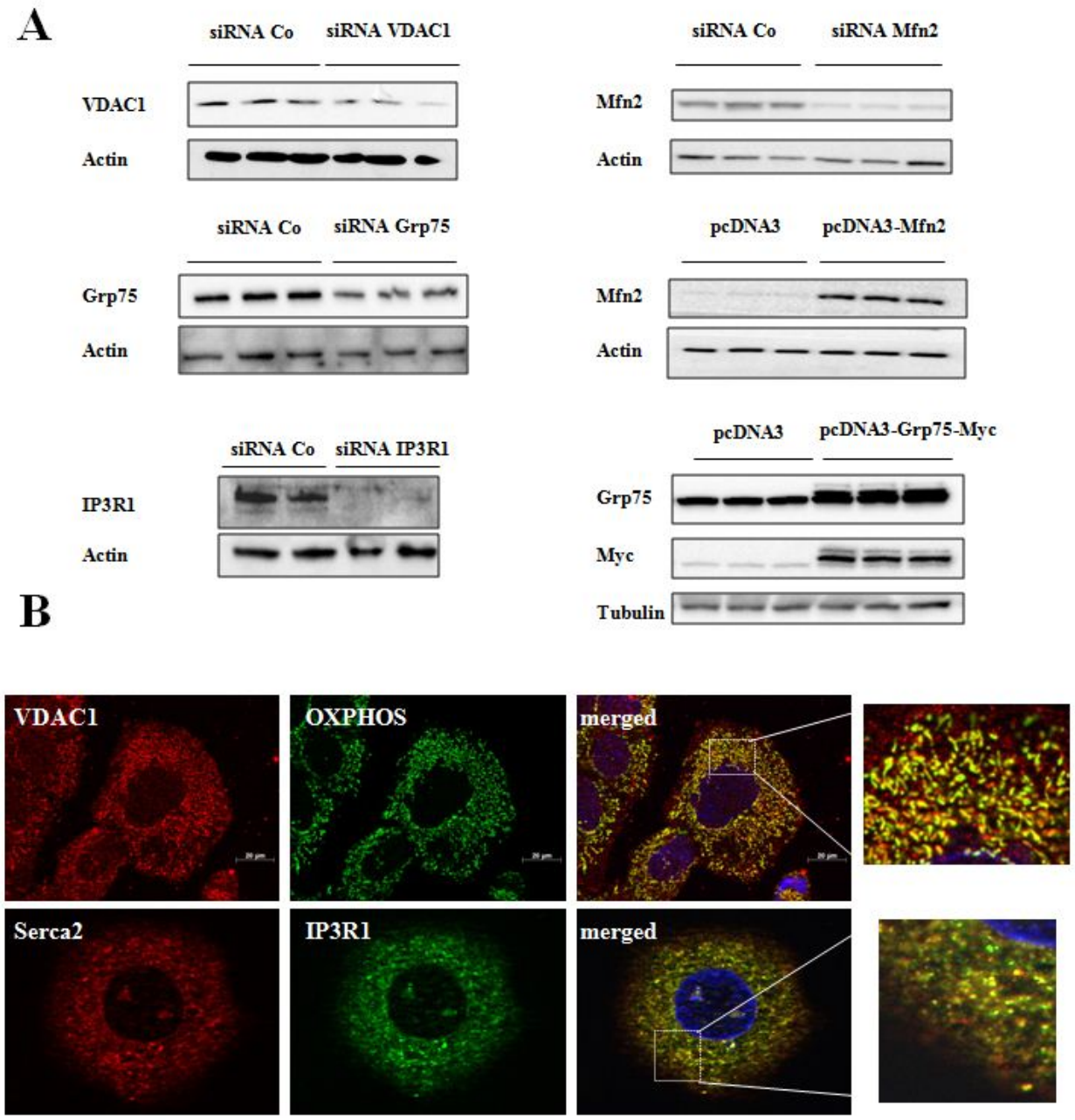

SUPPLEMENTARY DATA

Supplementary Figure 3. Visualization of the VDAC1/Grp75/IP3R1 complex by immuno-fluorescence. Nuclei appear in blue and mitochondrial and ER proteins are labelled in green or red, and the yellow colour on merged images illustrates co-localization between them (x63 and scale bar=20mm). At right, a zoom of merged images is shown. Co-localization is observed for VDAC1/IP3R1, Grp75/IP3R1 and VDAC1/Grp75 proteins, whereas it is not the case for ANT/IP3R1, ANT/Grp75 and Serca2/Grp75 proteins, indicating that the VDAC1/Grp75/IP3R1 Ca2+ channelling complex could be visualized by immuno-fluorescence.

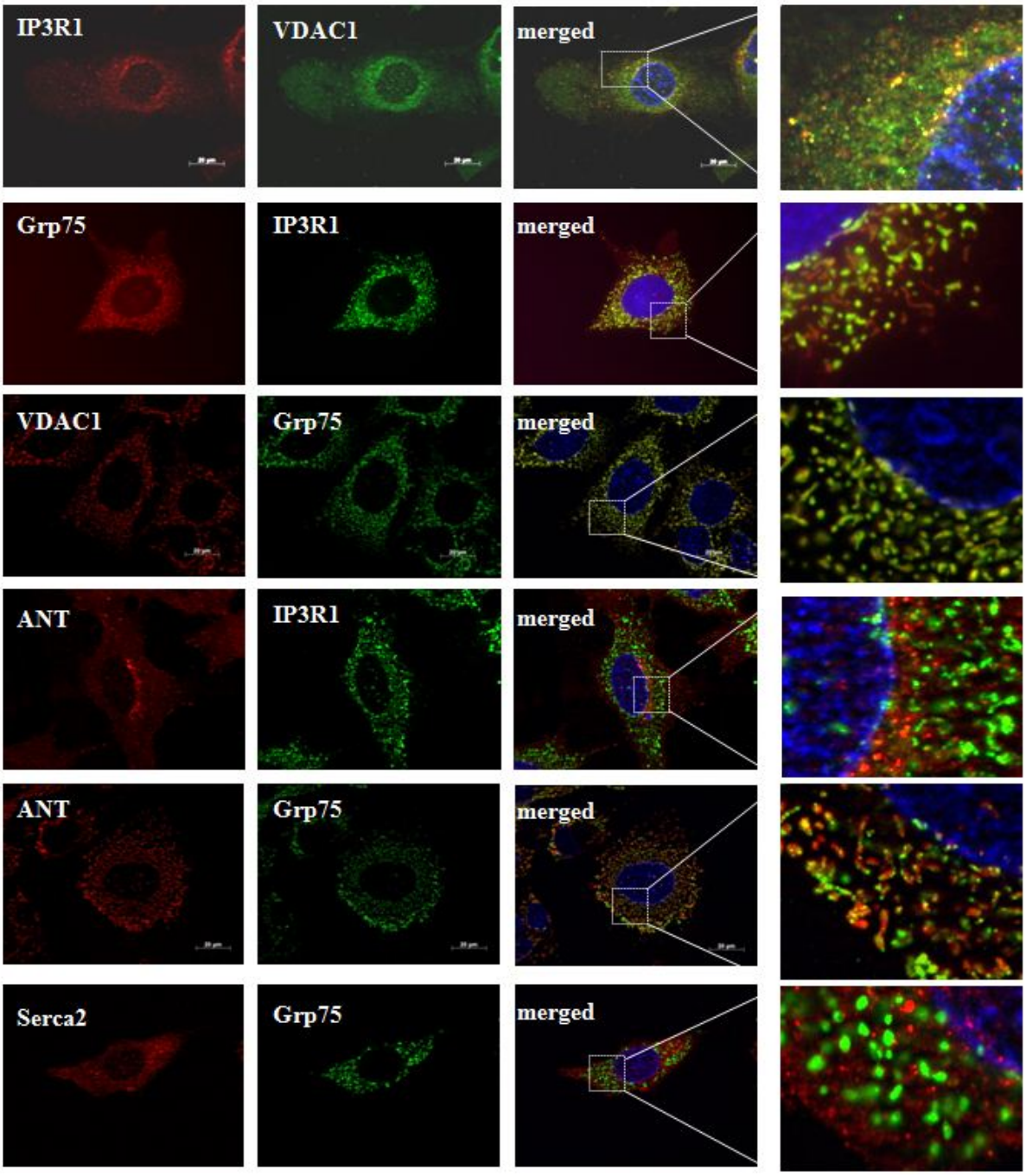

SUPPLEMENTARY DATA

Supplementary Figure 4. Visualisation of the VDAC1/Grp75/IP3R1 Ca^{2+} channelling complex by *in situ* proximity ligation assay (PLA). Visualisation of protein interactions by *in situ* PLA in HuH7 cells (x63 and scale bar=20mm). Nuclei appear in blue and interactions between the two targeted proteins are depicted in red. We show that VDAC1 interacts with both Grp75 and IP3R1, and that Grp75 interacts with IP3R1. As negative controls, we demonstrate that both VDAC1 and Grp75 did not interact with Serca2 (another ER membrane protein), and that the inner membrane mitochondrial protein ANT did not interact with IP3R1.

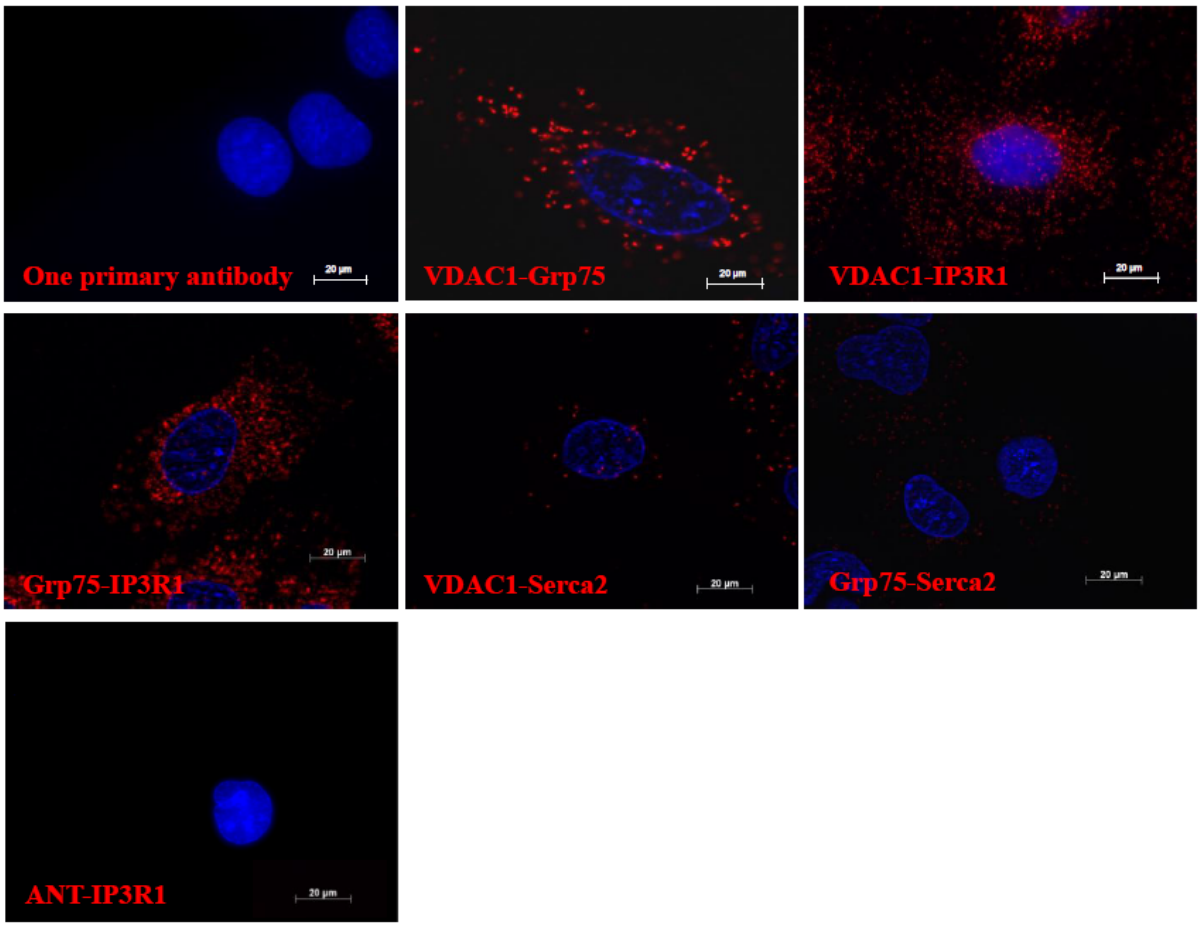

SUPPLEMENTARY DATA

Supplementary Figure 5. Inhibition of IP3R by Xestospongin C reduces ER-mitochondria interactions and alters insulin signalling. *In situ* PLA images (at left, x63 and scale bar=20μm) and quantitative analysis (at right) of VDAC1/IP3R1 interactions in HuH7 cells, treated or not for 18hours with either Xestospongin C (1μM),a specific inhibitor of IP3R, or with U73122 (1μM), an inibitor of IP3 production by PLC. Both Xestospongin C and U73122 treatments reduce VDAC1/IP3R1 interactions in HuH7 cells. *p<0.05 vs. untreated condition, n=3. B) Representative Western blot (at bottom) and quantitative analysis (at top) of insulin-stimulated PKB phosphorylation in HuH7 cells treated or not with Xestospongin C. Xestospongin C treatment reduces insulin-stimulated PKB phosphorylation in HuH7 cells. *p<0.01 vs. respective control (Co) without insulin. # p<0.05 vs. respective Co with insulin, n=3.

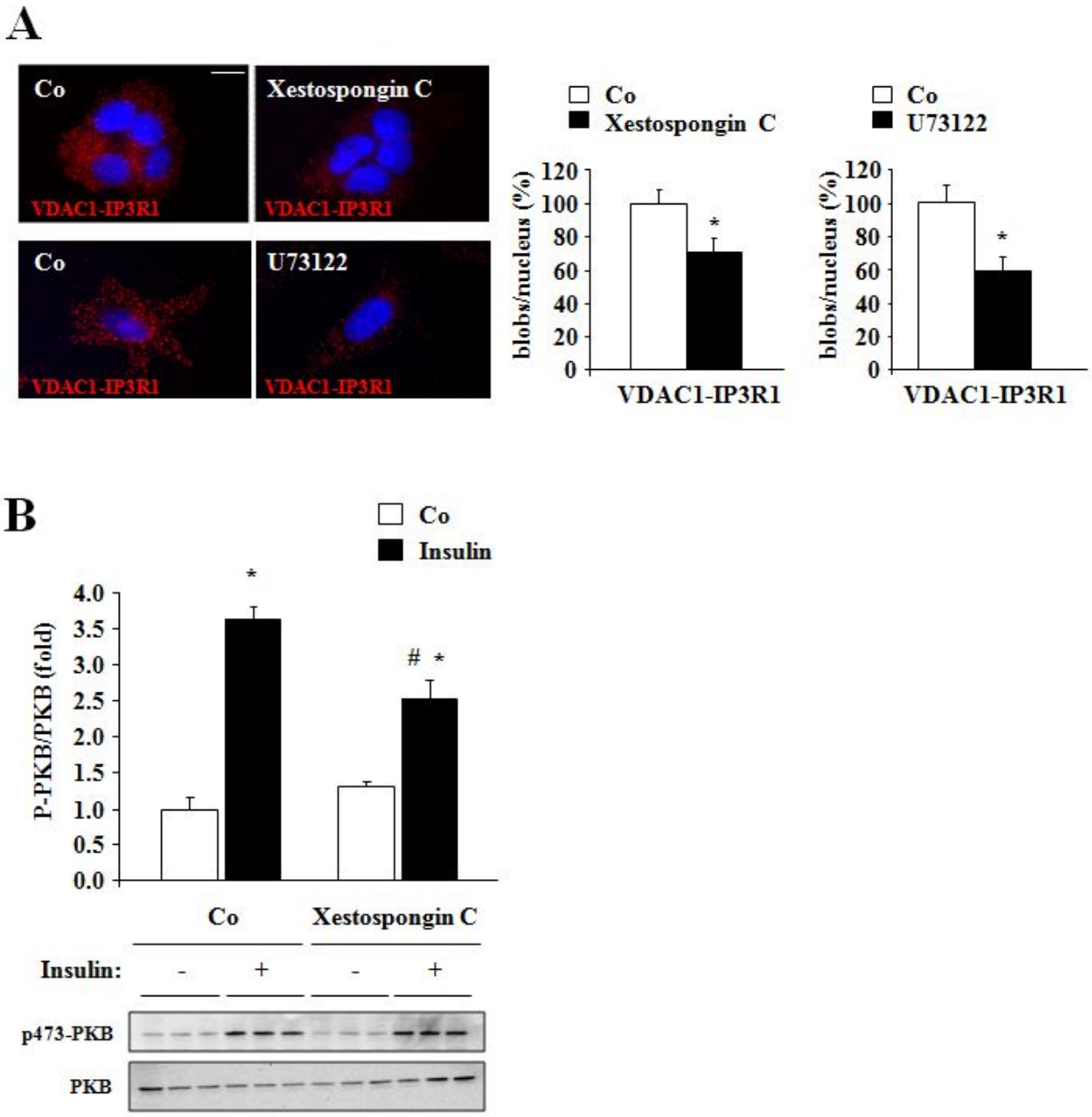

SUPPLEMENTARY DATA

Supplementary Figure 6. Validation of the cellular fractionation of liver. Mouse liver homogenate was fractioned into pure mitochondria (pM), mitochondria-associated endoplasmic reticulum membranes (MAM) and endoplasmic reticulum (ER) fractions, which are analyzed by electronic microscopy. For structural analysis, pellets of pure mitochondria (pM), ER and MAM from WT liver were fixed in 2% glutaraldehyde for 2h at 4°C, postfixed in 1% osmium tetroxide for 1h at 4°C, dehydrated and embedded in Epon. The tissue was then cut using a RMC/MTX ultramicrotome (Elexience) and ultrathin sections (60-80nm) were mounted on copper grids, contrasted with 8% uranyl acetate and lead citrate, and observed with a Jeol 1200 EX transmission electron microscope (Jeol LTD) equipped with MegaView II high resolution TEM camera. Analysis was performed with Soft Imaging System (Eloïse SARL).

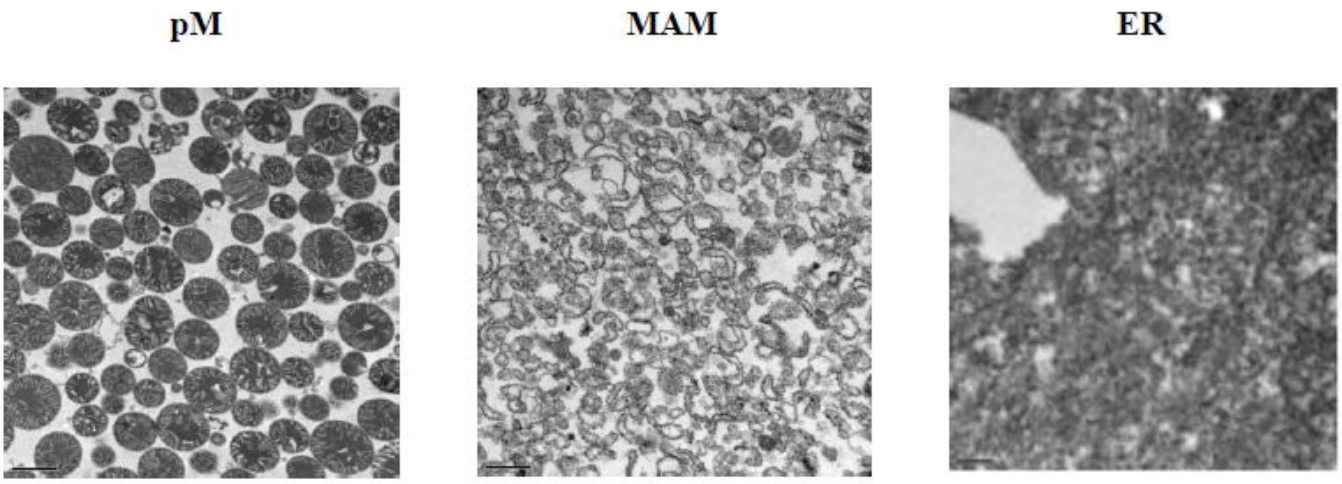

SUPPLEMENTARY DATA

Supplementary Figure 7. MAM are a hub of insulin signalling proteins in hepatocytes. A) Overnight fasted mice were injected with insulin (2mU/g of body weight) for 20 min. Representative Western blots (at left) and quantitative analysis (at right) of insulin-stimulated PKB phosphorylation in liver homogenates or MAM fractions of mice. Note that two parts of a same gel originally separated by irrelevant lanes are shown. Western blots of CD81 and Grp75 validate the absence of plasma membrane proteins and the enrichment of Grp75 in MAM fractions. *p<0.00; **p<0.0001 vs. control (Co), #p<0.0001 vs. Homogenat with insulin, n=3. B) Representative PLA images (at top, x63 and scale bar=20μm) and quantitative analysis of PKB/IP3R1, pS473-PKB/IP3R1 and VDAC1/IP3R1 interactions (at bottom) in HuH7 cells treated or not with insulin. HuH7 cells were depleted of serum for 3 hours before stimulation with insulin (10^{-7}M, 15min.). *p<0.05 vs. Co, n=3 independent experiments.

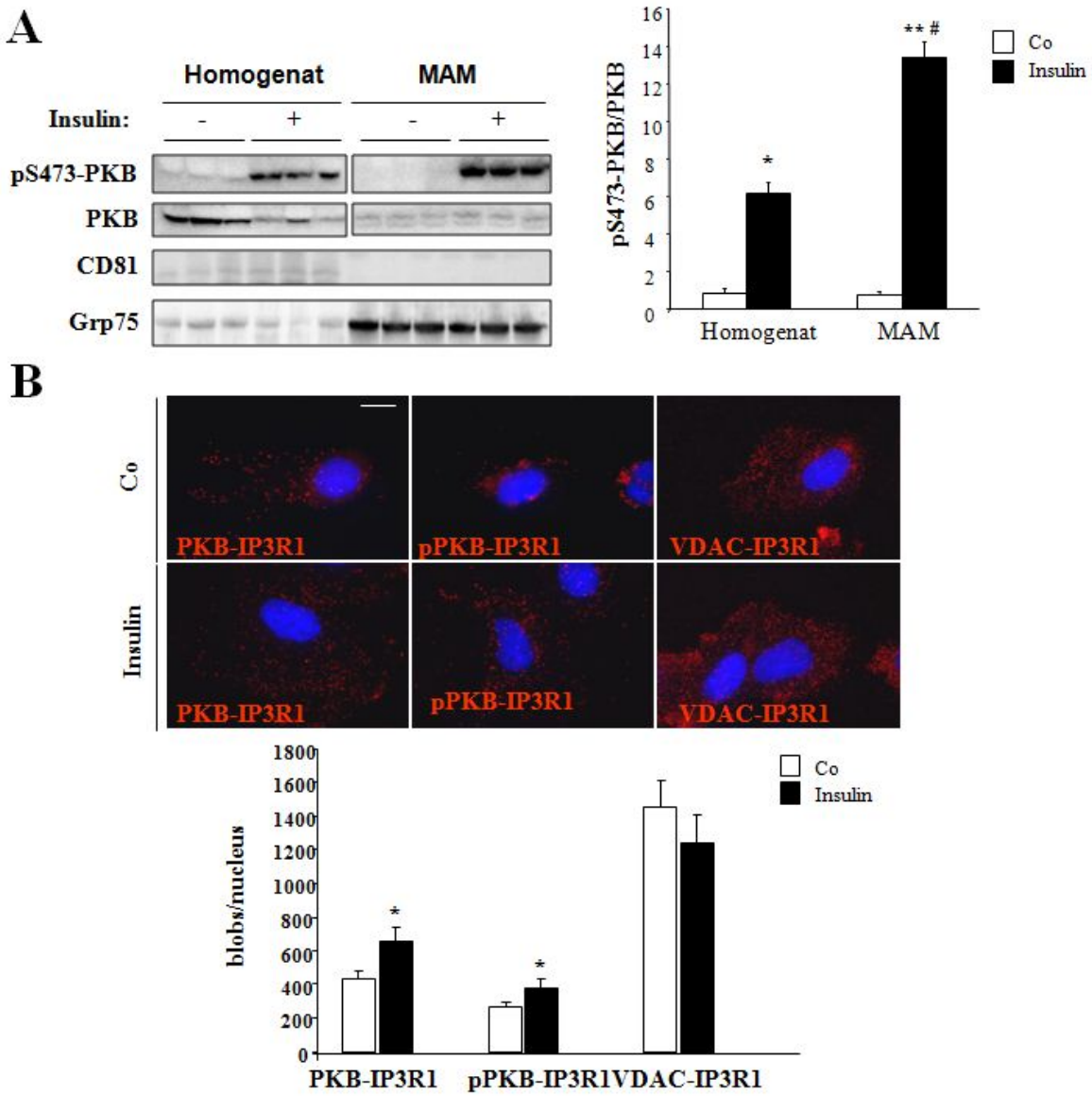

SUPPLEMENTARY DATA

Supplementary Figure 8. Loss of CypD disrupts interaction of cypD with IP3R1 in hepatocytes and induces insulin resistance. A) In situ PLA images (at left, x63 and scale bar=20μm) and quantitative analysis (at right) of CypD/IP3R1 interactions in primary hepatocytes of WT and CypD-KO mice. *p<0.005 vs. WT, n=3. B) Insulin tolerance test (0.75mU/g body weight) were performed on 6-hour fasted wt, CypD-KO and metformin-treated CypD mice. Results are expressed as mean ± SEM, n=7-10.

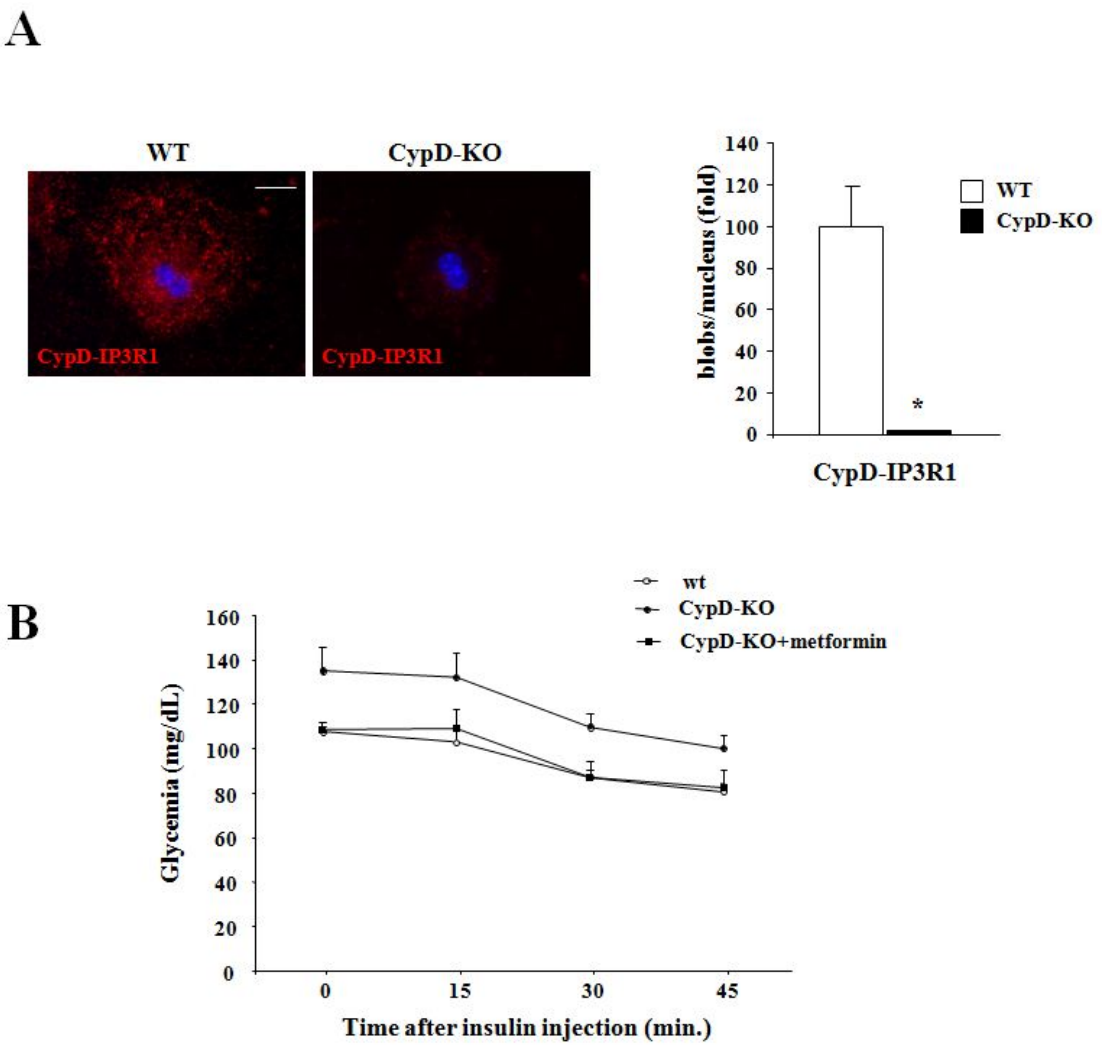

SUPPLEMENTARY DATA

Supplementary Figure 9. Glucose homeostasis of genetically- and nutritionally-induced obese and diabetic mice. A-D) For glucose tolerance test (GTT, A and C) and insulin tolerance test (ITT, B and D), wt and diabetic mice were fasted for 6 hours after 8 am. Then, glucose (2mg/g body weight) or insulin (0.75mU/g body weight) were injected i.p. and blood glucose levels were monitored at the indicated time points. A-B) GTT and ITT were performed on wt and ob/ob mice. C-D) GTT and ITT were performed on SD, HFHSD and Rosiglitazone-treated HFHSD mice. Results are expressed as mean ± SEM, n=10.

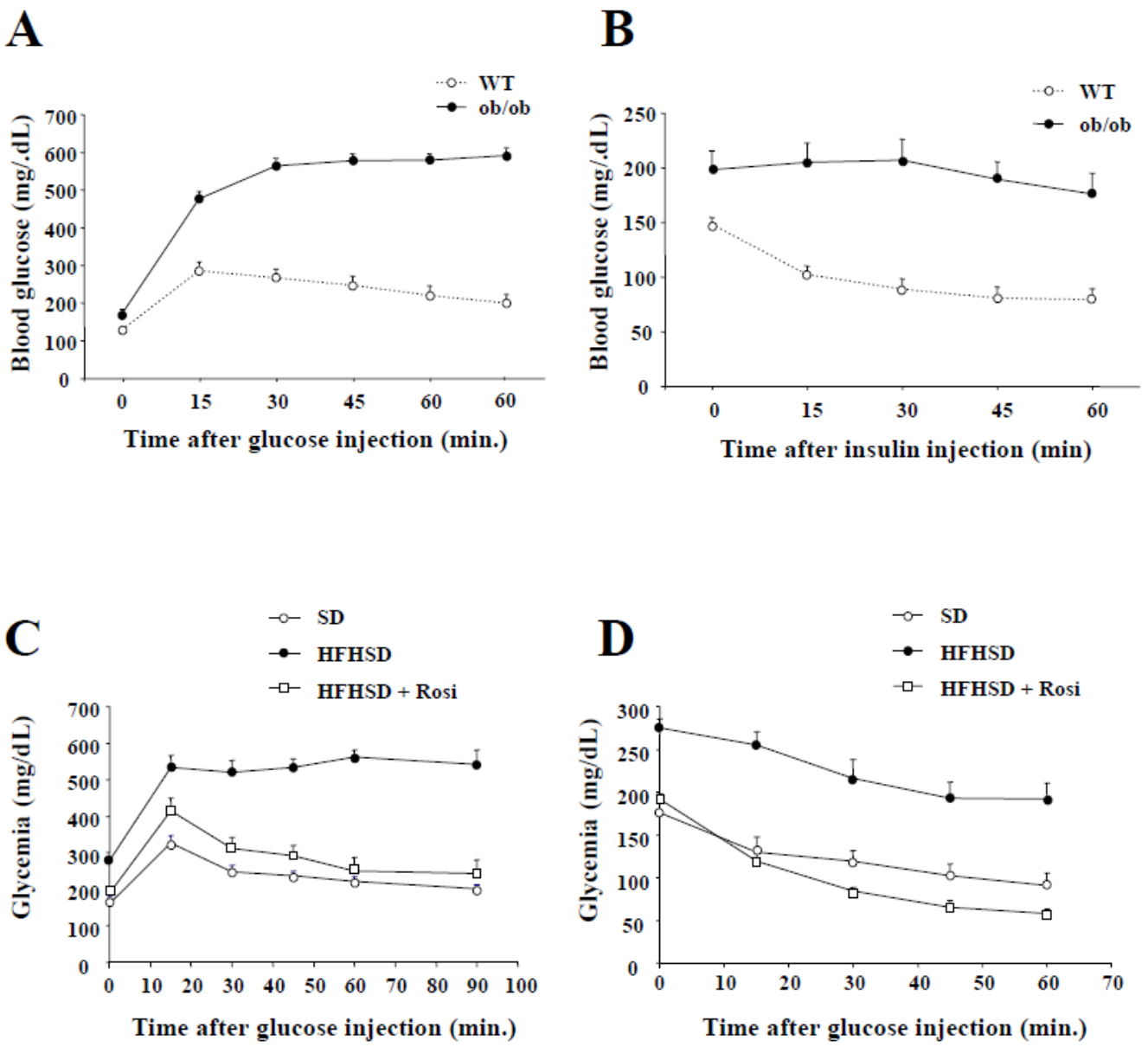

SUPPLEMENTARY DATA

Supplementary Figure 10. Validation of CypD overexpression in primary hepatocytes of HFHSD mice. Primary hepatocytes of HFHSD mice were infected with adenovirus encoding for GFP (Ad-GFP, as control) or cyclophilin D (Ad-CypD) for 36 hours. Validation by Western blot of the overexpression of CypD in infected primary hepatocytes of HFHSD mice. *p<0.05.

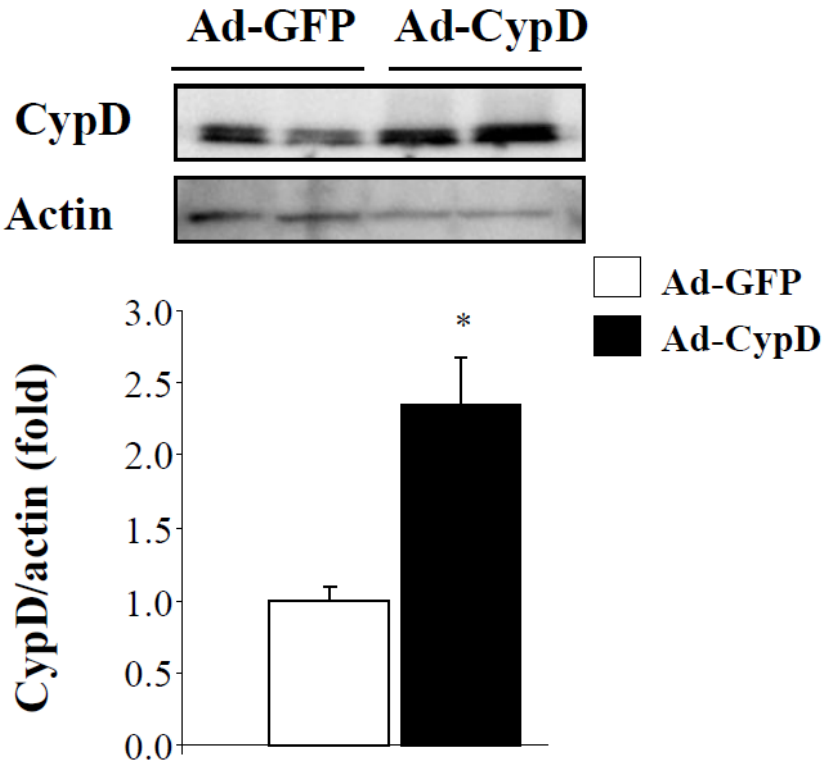

SUPPLEMENTARY DATA

Supplementary Figure 11. Modulation of MAM integrity impacts ER stress in HuH7 cells. ER stress markers were measured by real-time RT-PCR in HuH7 cells overexpressing or silenced for Mfn2 and Grp75. Results are expressed as mean ± SEM, n=3. *p<0.05 and **p<0.01vs. respective controls.